4-Terminal CPV Module Capable of Converting Global Normal Irradiance into Electricity

Juan F. Martínez[1, a)], Marc Steiner[1], Maike Wiesenfarth[1] and Frank Dimroth[1]

[1]*Fraunhofer Institute for Solar Energy Systems ISE, D-79110 Freiburg, Germany*

[a)]Corresponding author: juan.francisco.martinez.sanchez@ise.fraunhofer.de

Abstract. This paper investigates the outdoor performance of a new kind of hybrid concentrator photovoltaic module. The concept which we name, EyeCon, uses an array of Fresnel lenses to concentrate direct irradiance onto III-V four-junction solar cells while a large-area silicon cell absorbs diffuse sunlight and also acts as a heat distributing substrate. The preliminary results show that under a high ratio of direct to global irradiance (> 0.9) the concept is capable to convert up to 36.8 % of the global solar resource rather than just the direct beam. Moreover at a low ratio of direct to global irradiance (0.57) the hybrid module generates 30 % additional power with respect to the array of concentrator four-junction solar cells alone. The Eyecon module is applicable to all regions of the world and allows reaching the highest energy yield per module area of any PV technology.

INTRODUCTION

Concentrator photovoltaic (CPV) modules are already capable of converting 38.9 % [1] of the direct normal irradiance (DNI) into electricity. However due to the use of concentrator optics with inherently narrow acceptance angles (< 1°) they have only been able to compete with flat-plate PV modules in locations of high direct normal irradiation (> 2000 kWh/m^2/a) [2]. This is because even in suitable regions for conventional CPV the unabsorbed diffuse sunlight amounts to 10-30 % of the global normal irradiance (GNI), see Fig.1 bottom.

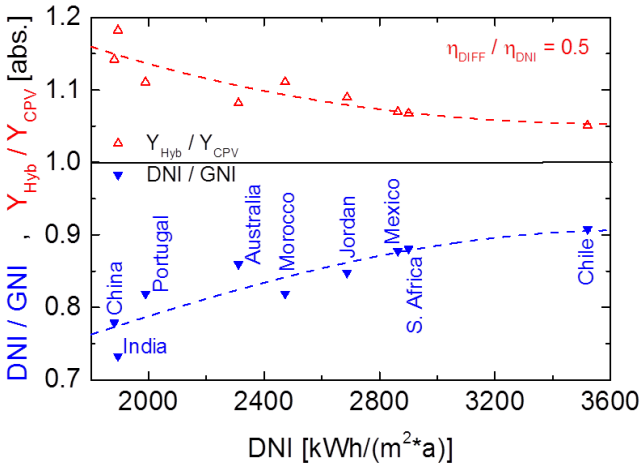

FIGURE 1. (Top) Calculated energy yield ratio between hybrid and conventional CPV modules (open triangles) assuming a conversion efficiency of 19 % for diffuse- and 39 % for direct light. (Bottom) The average ratio of direct/global irradiance is shown as a function of direct normal irradiation (solid triangles) to depict the average diffuse sunlight component for different sites in the world. Calculations are based on SolarGIS long term yearly average data.

On the other hand silicon (Si) solar cells have decreased their price tremendously in the past years [3]. This makes them an interesting candidate for integration with CPV into a hybrid module that converts global rather than only direct irradiance. If we assume that the Si cell converts diffuse irradiance with half the efficiency at which the CPV cell converts DNI (e.g. η_{DIFF} = 19 % and η_{DNI} = 38 %), we can calculate the expected energy yield of the hybrid module, Y_{Hyb}, in comparison with conventional CPV, Y_{CPV} (Fig. 1 top). Such increase is in the range of 5 % for regions like Chile with extremely high DNI/GNI > 0.9, and 20 % in locations like India with DNI/GNI around 0.7. Recent reports in the literature showed an increase in the power output at high DNI/GNI (0.924) in the range of 3.4 % for a 1000x micro-CPV module that uses plano-convex lenses, triple-junction solar cells and interdigitated back contact (IBC) Si cells mounted on a copper backplane [4]. An even higher increase in power output of 39 % (at DNI/GNI > 0.75) and 63 % (at 0.4 < DNI/GNI < 0.5) was reported for a 200x miniature module using PMMA lenses, triple-junction cells and a bifacial Si cell encapsulated between two glass plates [5]. In this particular example the additional generation of power is significantly higher compared to Fig. 1 due to the albedo received by the bifacial Si cell.

CPV/FLAT-PLATE HYBRID CONCEPT

The idea of combining a concentrator high-efficiency solar cell with a flat-plate PV cell in order to enhance CPV power output was first patented in 2009 by Benitez et al. [6]. Later in 2014 Meitl et al. also patented the same idea with the distinction that they proposed a 2-terminal device [7]. The hybrid concept investigated in this paper (see Fig. 2) uses silicone-on-glass Fresnel lenses to concentrate DNI on a III-V four-junction solar cell with peak conversion efficiency in the range of 45 %. Additionally, a large area Si solar cell is integrated underneath as substrate to absorb the non-concentrated diffuse radiation while it also distributes heat radially to enable passive cooling. This way the additional cost of the silicon cell is leveraged by the removal of the metal heat spreader typically used in conventional CPV technology. Finally, in order to extract maximum power from both cells we use a 4-terminal configuration where CPV and Si cell circuits are independent from each other to avoid mismatch current/voltage losses due to fluctuating spectral conditions.

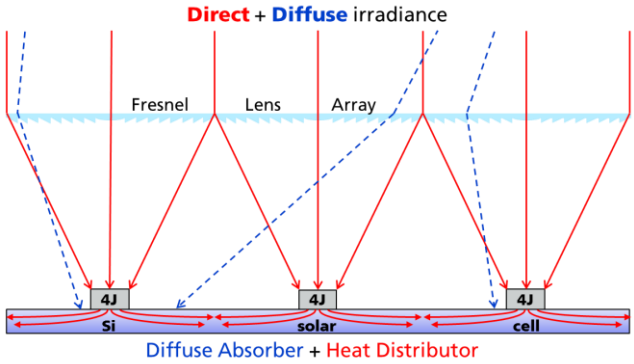

FIGURE 2. Schematic diagram of the hybrid CPV module concept where a Fresnel lens concentrates direct irradiance (solid lines) onto a four-junction solar cell while a large area Si cell positioned underneath acts as a substrate which absorbs diffuse irradiance (dashed lines) and also distributes heat radially in order to passively cool the CPV cells.

MODULE ARCHITECTURE

The architecture of the module used for outdoor testing is presented in Fig. 3. On the left side we see the inside of the module where the cell-stack is fixed onto a glass baseplate using standard ethylene-vinyl acetate (EVA) lamination. The cell-stack itself is made up of nine CPV solar cell assemblies mechanically attached to the surface of one Si IBC cell with a dielectric adhesive. The dielectric is a ceramic filled epoxy glue with thermal resistance below 150 mm^2*K/W in order to facilitate heat transfer from the CPV cells to the Si IBC cell. Each assembly comprises a copper back contact (12 mm x 4 mm) on which the four-junction cell (d = 3 mm) is soldered together with a bypass diode that is thin-wire bonded to the cell's front contact. The CPV array is achieved by successively heavy-wire bonding back and front contacts until they are interconnected to the bottom junction box. The diffuse

sunlight absorbing/heat distributing substrate is a commercially available pseudo-squared Si IBC cell (125 mm x 125 mm) that is independently interconnected to the top junction box. In this manner we obtain a 4-terminal submodule that is surrounded by a glass frame with an inner mirror finish (82 % reflective) that blocks external light from entering the module but reflects internal light to reproduce the optical boundary of a larger size module. On the right side of Fig. 3 we observe the finished prototype where a 3 x 3 Fresnel lens array with an aperture of 144 cm^2 yields a geometric concentration of 226x.

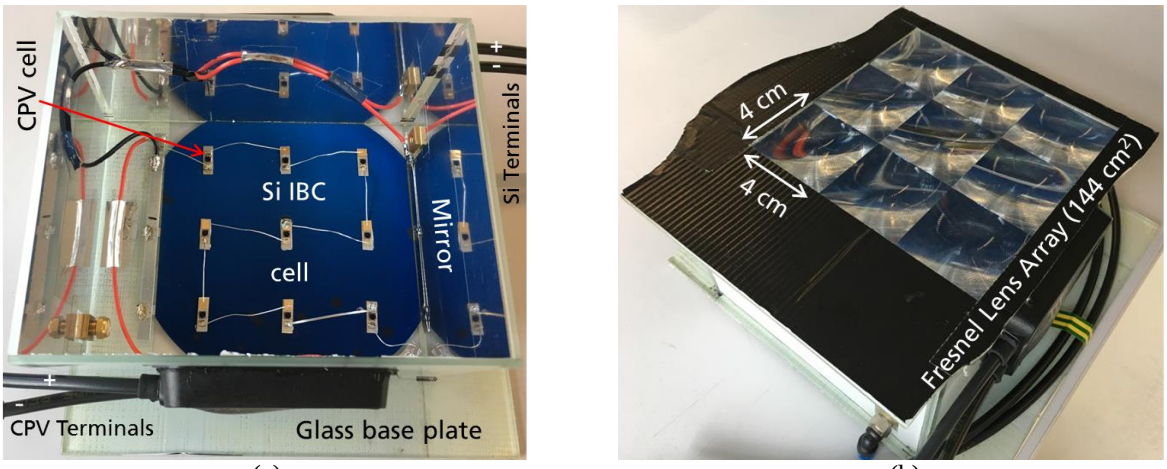

(a) (b)

FIGURE 3. (a) Photograph of the inside and (b) outside of the hybrid CPV submodule architecture.

OUTDOOR EVALUATION

In the following subsections we shall present the outdoor evaluation of the hybrid CPV submodule regarding absorption of diffuse irradiance by the Si cell, GNI based efficiency, power output and power gain of the concept under high and average DNI/GNI ratios.

Absorption of Diffuse Irradiance

In this subsection we investigate the optical interactions between Fresnel lens and cell-stack in order to quantify the amount of irradiance absorbed by the Si cell (Irr_{Si}). Figure 4 shows on the left side a photograph of the hybrid cell-stack during outdoor operation where we observe brighter squared regions on the Si cell around the CPV cells.

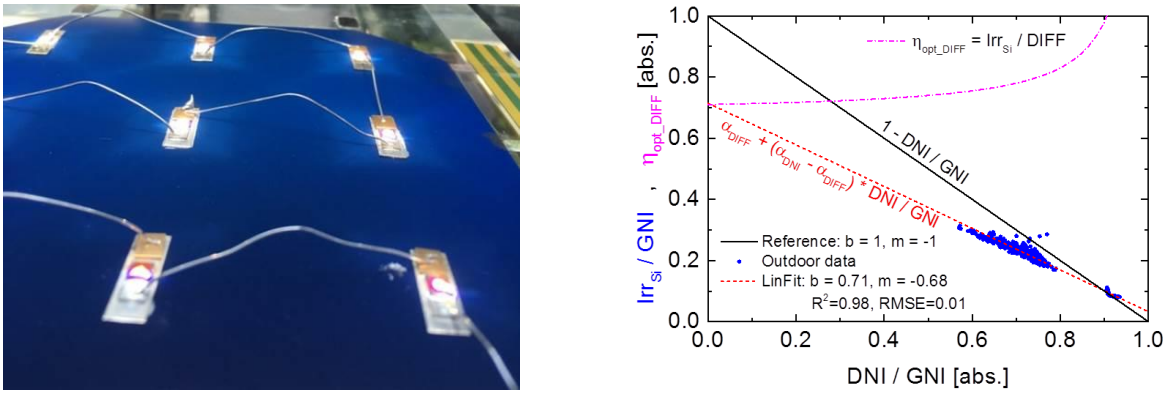

(a) (b)

FIGURE 4. (a) Photograph of the hybrid cell-stack during outdoor operation (b) Ratio of absorbed irradiance by the Si cell (Irr_{Si}) and diffuse irradiance (DIFF) optical efficiency as a function of DNI/GNI measured in 6/2016 and 3/2017 in Freiburg, Germany.

This indicates that the photon flux is more intense at these locations. We assume that this higher intensity region is due to reflected direct sunlight that the draft facets of the Fresnel structure were unable to refract onto the CPV cell. Therefore in equation 1 we define Irr_{Si} as the sum of a diffuse (α_{DIFF}) and a direct irradiance fraction (α_{DNI}) with DIFF abbreviating GNI-DNI

$$Irr_{Si} = \frac{I_{SC}}{6.03\ mA{\cdot}m^2/W} = \alpha_{DIFF} \cdot DIFF + \alpha_{DNI} \cdot DNI \quad (1)$$

where the value of Irr_{Si} is calculated from the outdoor measured short-circuit current (I_{SC}) of the Si cell within the module and the constant 6.03 mA*m^2/W corresponds to the indoor measured current of the bare Si cell. Dividing equation 1 by GNI transforms the former multi-linear model into a linear one that only depends on DNI/GNI, as expressed in equation 2

$$\frac{Irr_{Si}}{GNI} = \alpha_{DIFF} + (\alpha_{DNI} - \alpha_{DIFF}) \cdot \frac{DNI}{GNI} \quad (2)$$

where α_{DIFF} = 0.71 ± 0.01 represents the value at DNI/GNI = 0 and (α_{DNI} - α_{DIFF}) = -0.68 ± 0.01 corresponds to the slope of the linear fit (red line) applied to the data (blue scatter) in the plot of Fig. 4. This inverse proportional relationship shows that Irr_{Si}/GNI decreases with DNI/GNI at a slower rate than expected as the Si cell absorbs 71 % of diffuse radiation (α_{DIFF}) plus 3 % of DNI (α_{DNI}). The black line represents the reference case, DIFF/GNI, where 100 % of diffuse radiation and 0 % of DNI is absorbed. Dividing equation 2 by DIFF/GNI yields the ratio Irr_{Si}/DIFF, i.e. the diffuse irradiance optical efficiency, η_{opt_DIFF} (magenta line). We observe in Fig. 4 that η_{opt_DIFF} has a minimum value of 71 % that increases as a function of DNI/GNI until the absorbed DNI compensates all losses of diffuse light at DNI/GNI = 0.9 where η_{opt_DIFF} = 100 %. In other words the solar resource on the silicon cell when DNI/GNI > 0.9 is always higher than expected purely from the diffuse radiation because some of the DNI is also reaching the Si cell and contributing to photocurrent.

Performance for High DNI/GNI Ratio

The definitions of the conversion efficiencies used to describe the outdoor performance of the hybrid module are presented in equation 3

$$\eta_{DNI} = \frac{P_{CPV}}{DNI} \quad , \quad \eta_{DIFF} = \frac{P_{Si}}{DIFF} \quad , \quad \eta_{GNI} = \frac{P_{Hyb}}{GNI} \quad (3)$$

where η_{DNI} , η_{DIFF} , η_{GNI} are the efficiencies at which DNI, DIFF and GNI are converted into electric power output by the CPV array (P_{CPV}), Si cell (P_{Si}) and hybrid module ($P_{Hyb} = P_{CPV} + P_{Si}$), respectively.

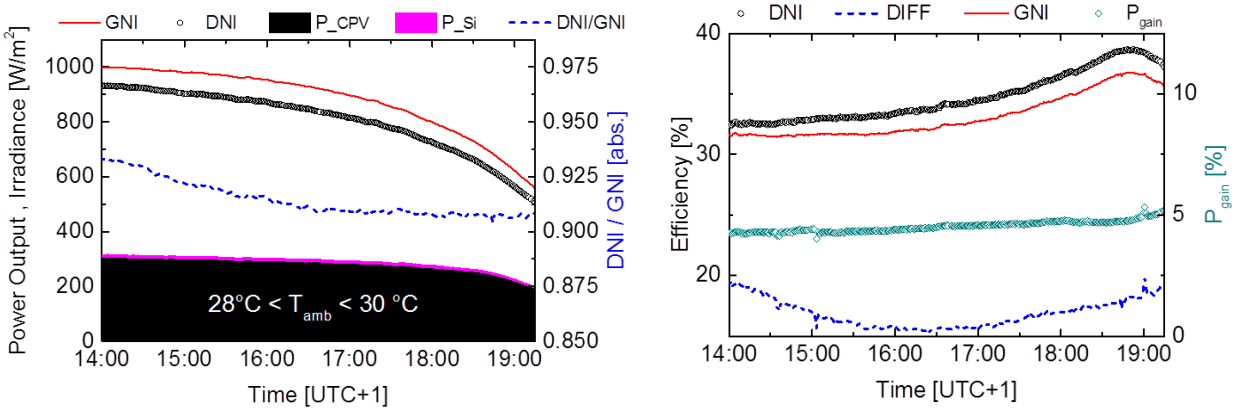

(a) (b)

FIGURE 5. (a) GNI, DNI, P_{Si}, P_{CPV}, DNI/GNI and (b) η_{DNI}, η_{DIFF}, η_{GNI}, P_{gain} time-series of the hybrid submodule tested in Freiburg, Germany during 6/2016 under DNI/GNI > 0.9.

On the left side in Fig. 5 we observe P_{CPV} (bottom area) and P_{Si} (stacked area) during a clear-sky summer day in Freiburg, Germany where DNI/GNI (dashed line) varied between 0.93 and 0.9 as GNI and DNI decreased continuously. The P_{Hyb} at GNI = 1000 W/m^2 reached 317 W/m^2 from which the CPV array contributed 304 W/m^2 and the Si cell 13 W/m^2.

As shown on the right side in Fig. 5, this corresponds to η_{DNI} = 32.7 %, η_{DIFF} = 18.3 % and η_{GNI} = 31.7 %. However as the direct spectrum became red-rich due to the increase of air mass, η_{DNI} rose to 38.9 % and η_{GNI} reached a maximum value of 36.8 % at GNI = 650W/m^2. At the same time η_{DIFF} decreased from 18.3 % to 15.2 % due to η_{opt_DIFF} decreasing with DNI/GNI; however it recovered to 17.4 % as the Si cell cooled down. Overall the average gain in power by the silicon cell was 5 %.

Performance for Average DNI/GNI Ratio

The submodule performance during more hazy conditions where DNI/GNI (dashed line) varied between 0.57 and 0.78 is depicted in Fig. 6. On the left plot we observe that the fluctuation of P_{CPV} (bottom area) and P_{Si} (stacked area) is correlated to the variation of DNI (scatter plot) and GNI (solid line). However in this case the Si cell contributed in average, (33 ± 4) W/m^2, a larger P_{Hyb} fraction than before, while the CPV array still generated, (192 ± 37) W/m^2, the largest contribution to the overall power output of the module.

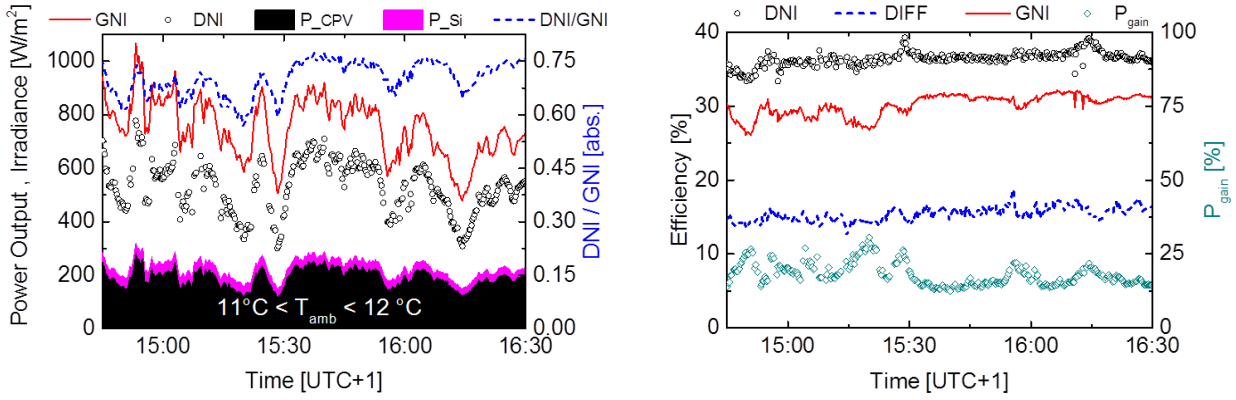

(a) (b)

FIGURE 6. (a) GNI, DNI, P_{Si}, P_{CPV}, DNI/GNI and (b) η_{DNI}, η_{DIFF}, η_{GNI}, P_{gain} time-series of the hybrid submodule tested in Freiburg, Germany during 3/2017 under 0.57 < DNI/GNI < 0.78.

On the right graph we observe a η_{DNI} = (36.4 ± 1) %, η_{DIFF} = (15.6 ± 1.3) % and η_{GNI} = (30.3 ± 1.5) %. This corresponds to a P_{gain} that fluctuates between 12.1 % and 30.6 %. Although the total power output is lower than for high DNI/GNI cases, the module generated in average (17.7 ± 1.7) % additional power thanks to the Si cell. This confirms the positive effect of the hybrid approach under conditions with average diffuse radiation.

Power Gain (P_{Si} / P_{CPV})

In order to evaluate the additional power generation of the hybrid concept in comparison to CPV alone, we define the quantity power gain, P_{gain}, as the ratio between P_{Si} and P_{CPV} where substitution of their equivalents from equation 3 leads to equation 4.

$$P_{gain} = \frac{P_{Si}}{P_{CPV}} = \frac{\eta_{DIFF}}{\eta_{DNI}} \cdot \frac{DIFF}{DNI} \quad (4)$$

In Fig. 7 we see that P_{gain} holds a linear relationship with DIFF/DNI where the slope corresponds to the ratio between efficiencies, η_{DIFF}/η_{DNI} = 0.4. The data shows that although DIFF and DNI vary over time during outdoor operation, the hybrid module converts diffuse and direct irradiance at a fixed ratio.

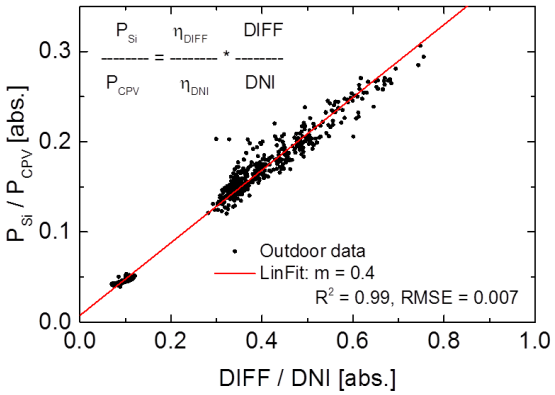

FIGURE 7. Power gain (P_{Si}/P_{CPV}) of the hybrid module with respect to the CPV array as a function of DIFF/DNI with DIFF = GNI-DNI. The measurements were performed during 6/2016 and 3/2017 in Freiburg, Germany.

In Table 1 we show that for regions with direct normal irradiation above 1900 kWh/m^2*a, the expected annual power gain is around 5 % for the most suitable CPV location in Chile and 15 % for a less favorable site e.g. in India. However it must be remarked that at any location extremely cloudy days occur throughout the year where conventional CPV modules would have no output, thus the power generated by the silicon cell makes the hybrid system a more robust source of renewable energy.

TABLE 1. List of Power Gains as a function of DNI/GNI

DNI/GNI	P_{gain}	Region
0.91	5 %	Chile
0.82	10 %	Portugal
0.73	15 %	India
0.58	30 %	< 1900 kWh/(m^2*a)

SUMMARY

We have demonstrated the outdoor performance of a 226x hybrid CPV submodule capable to convert direct and diffuse irradiance by using Fresnel lenses, III-V four-junction concentrator solar cells and a silicon interdigitated back contact cell. During a clear sunny day in Freiburg, Germany (DNI/GNI > 0.9) the prototype achieved a GNI-based efficiency of 31.7 % at 1000 W/m^2 and up to 36.8 % at 650 W/m^2. This corresponds to 5 % additional power generated by the silicon cell with respect to the CPV array. Under hazy conditions (0.57 < DNI < 0.78) the average GNI-based efficiency was (30.3 ± 1.7) % and the additional generated power was 30.6 % at DNI/GNI = 0.57 and 12.1 % at DNI/GNI = 0.78. These results show that the hybrid concept is able to achieve GNI-based efficiencies above 36 % on ideal days for CPV, whereas on less sunny days it generates in average 17.7 % additional power. Furthermore, the ability to capture diffuse irradiance by the integrated silicon cell was investigated and it was shown that it absorbs more than 71 % of the diffuse sunlight that the Fresnel lens does not concentrate onto the CPV solar cells. Further work to continue characterizing and improving the outdoor performance of the concept is on-going.

ACKNOWLEDGMENTS

The authors want to acknowledge the support of SOITEC in the fabrication of four-junction concentrator solar cells and all colleagues of the “III-V Photovoltaics and Concentrator Technology” and the “Module Technology” departments at Fraunhofer ISE for their contributions and in particular the latter for their support laminating silicon solar cells. This work was partly supported by the National Council of Science and Technology (CONACYT) and by the Mexican Secretary of Energy (SENER). The authors are responsible for the contents of this paper.

REFERENCES

1. S. van Riesen, M. Neubauer, A. Boos, M. M. Rico, C. Gourdel, S. Wanka, R. Krause, P. Guernard, and A. Gombert in *AIP Conference Proceedings 1679* (2015), Vol. 1679, p. 100006.
2. S. P. Philipps, A. W. Bett, K. Horowitz, and S. Kurtz, *Current Status of Concentrator Photovoltaic (CPV) Technology* (2017).
3. R. Fu, D. Feldman, R. Margolis, M. Woodhouse, and K. Ardani, U.S. Solar Photovoltaic System Cost Benchmark: Q1 2017 (2017).
4. K.-T. Lee, Y. Yao, J. He, B. Fisher, X. Sheng, M. Lumb, L. Xu, M. A. Anderson, D. Scheiman, S. Han, Y. Kang, A. Gumus, R. R. Bahabry, J. W. Lee, U. Paik, N. D. Bronstein, A. P. Alivisatos, M. Meitl, S. Burroughs, M. M. Hussain, J. C. Lee, R. G. Nuzzo, and J. A. Rogers, Proceedings of the National Academy of Sciences of the United States of America **113**, E8210-E8218 (2016).
5. N. Yamada and D. Hirai, Prog. Photovolt., Res. Appl. **24**, 846 (2016).
6. P. Benitez, J. C. Miñano, and R. Alvarez, Photovoltaic concentrator with auxiliary cells collecting diffuse radiation, US 2010/0126556 A1 (2009).
7. M. Meitl, J. Carr, and K. Schneider, Power augmentation in concentrator photovoltaic modules by collection of diffuse light, US 2014/0261627 A1 (2014).